Tetraphosphonic acid as eco-friendly corrosion inhibitor on carbon steel in 3 % NaCl aqueous solution

S. Saker · N. Aliouane · H. Hammache · S. Chafaa · G. Bouet

Abstract The inhibition activity of a new tetraphosphonic acid (TPA), 2-hydroxy-5-[4-hydroxy-3,5-bis(phosphonomethyl) benzyl]-3-(phosphonomethyl)benzylphosphonic acid, for carbon steel in aerated 3 % NaCl solution, at 1000 rpm, was investigated using open circuit potential (OCP), potentiodynamic polarizations, and electrochemical impedance spectroscopy (EIS) to evaluate the TPA inhibition efficiency. The steel surface was also examined by SEM observations and energy-dispersive X-ray (EDX) analysis. The inhibition efficiency increased with TPA increasing concentration up to 10^{-3} mol L^{-1} where the highest inhibition efficiency (88 %) was obtained. The thermodynamic parameters—adsorption equilibrium constant, standard free energy, and activation energy—were calculated to determine the corrosion inhibition mechanism. Results from potentiodynamic polarization and electrochemical impedance spectroscopy revealed the mode of inhibitive action and adsorption of inhibitor molecules. Further, surface morphological examination supports the protective film formation by TPA on carbon steel surface. Inhibitor adsorption was spontaneous ($\Delta G < 0$), supported the physical/chemical adsorption mechanism, and obeyed to the Langmuir adsorption isotherm.

S. Saker · N. Aliouane · H. Hammache
Laboratoire d'Electrochimie, de Corrosion et de Valorisation Energétique, Département de Génie des Procédés, Université de Bejaia, 06000 Béjaia, Algérie

S. Chafaa
Laboratoire d'Electrochimie des Matériaux Moléculaires et des Complexes, Faculté des Sciences de l'Ingénieur, Université de Sétif, Sétif, Algérie

G. Bouet (✉)
UFR des Sciences Pharmaceutiques et d'Ingénierie de la Santé, Laboratoire SONAS EA 921, SFR QUASAV 4207, UNAM, Université d'Angers, 16 Boulevard Daviers, 49045 Angers Cedex, France
e-mail: gilles.bouet@univ-angers.fr

Introduction

Carbon steel has been one of the most important and widely used materials, playing a central role as basic material for the metallurgical industries. There are various techniques to protect carbon steel against corrosion in rough environments [1]. The use of corrosion inhibitors is one of the most economical and practical method to reduce the corrosive attack of the environment on carbon steel surface [2]. Some organic compounds were found to be effective corrosion inhibitors for many metals and alloys. The adsorption of inhibitors takes place through heteroatoms such as nitrogen, oxygen, phosphorus, and sulfur, as well as through triple bounds or aromatic rings. Nowadays, due to restrictive laws concerning the environment, most attention has been focused on the use of non-toxic organic compounds such as phosphonates [3, 4].

Phosphonates are molecules containing one or more R-$PO(OH)_2$ groups. These compounds are used worldwide in a broad spectrum of applications, including household and industrial detergents [5–7], industrial water treatment [8, 9], industrial cleaners, and enhanced oil recovery operations. This class of products also finds applications in medicinal chemistry as antiviral agents, in such a way that they can be considered as analogs of natural pyrophosphates [10–12]. Phosphonates and their derivatives were originally introduced in water treatment field as a scale control agent [13, 14], but now they are also widely used as corrosion inhibitors [15, 16].

Compounds which contain the phosphonate functional group play an important role in the corrosion protection of

metal in concrete, coating, rubber blends, acid cleaners, and antifreeze coolants [17]. Recently, their effect on the corrosion of carbon steel in deaerated delivery water at 90 °C has been studied, showing that introduction of phosphonates reduced the susceptibility of steel to local corrosion [18].

The adsorption of phosphonocarboxylic acid salts (monophosphonates) onto a carbon steel surface leads to the formation of an adherent protective film on the metal which acts like a barrier to aggressive ions such as chlorides [19, 20]. Other phosphonic acids like nitrilotris(methylenephosphonic acid) (NTMP) were also tested as inhibitor of the cathodic reaction in a saturated $Ca(OH)_2$ solution [21]. 1-Hydroxyethylidene-1,1-diphosphonic acid (HEDP) is studied extensively and considered as a corrosion inhibitor with non-toxicity in cooling water [22–26]. The inhibiting action of these organic compounds is usually attributed to their interactions with the metal surface via their adsorption. The adsorption process depends on the nature as well as the surface charge of the metal to be inhibited, the adsorption mode, the inhibitor's chemical structure, and the type of the electrolyte solution.

The search for new, more efficient, more specific polyphosphonate compounds represents a considerable challenge and is of great interest in the field of environmental remediation.

The aim of this study was to investigate the inhibiting effect of a new tetraphosphonic acid compound, 2-hydroxy-5-[4-hydroxy-3,5-bis(phosphonomethyl)benzyl]-3-(phosphonomethyl) benzylphosphonic acid (TPA) shown in Fig. 1, on carbon steel corrosion in aerated 3 % NaCl solution at 1000 rpm. It was anticipated that TPA would be an effective corrosion inhibitor because it contains two phosphonic groups on each phenyl (Fig. 1) and so many binding molecules to increase the capacity of TPA to be adsorbed on the carbon steel surface.

Materials and methods

Chemicals

The tetraphosphonic acid (TPA) used was newly synthesized according to the procedure previously described by some of
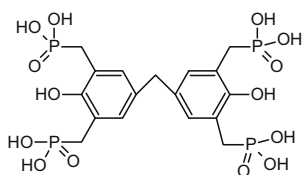

Fig. 1 Molecular structure of 2-hydroxy-5-[4-hydroxy-3,5-bis(phosphonomethyl)benzyl]-3-(phosphonomethyl)benzylphosphonic acid (TPA)

our group members [27, 28]. Its identity and purity were confirmed using ES-MS and NMR spectrometry.

TPA was added to the blank solution of 3 % NaCl (reagent grade) in aerated atmosphere, maintained at 25 °C, in $5 \cdot 10^{-5}$, 10^{-4}, $5 \cdot 10^{-4}$, and 10^{-3} mol L^{-1} concentrations, respectively. All the test solutions were adjusted to pH=7 using NaOH solution. In the study of the effect of temperature, experiments were carried out at 293, 303, 313, and 323 K.

Measurements

Electrochemical measurements were conducted using a three-electrode cell with a carbon steel work electrode, platinum auxiliary electrode, and a saturated calomel reference electrode (SCE). All potentials were given with reference to this electrode. Potentiodynamic polarization experiments were run using a VOLTALAB PGP 201 system potentiostat/galvanostat using "Voltamaster" software. The potential was scanned from open circuit potential (OCP) to +250 mV (vs. SCE) in the anodic region, and to −1000 mV (vs. SCE) in the cathodic region, with a scan rate of 1 mV/s. Electrochemical impedance spectroscopy (EIS) measurements were performed using an Autolab PGSTAT30 potentiostat/galvanostat. The impedance spectra were recorded at the open circuit potential (OCP) using 10 mV sinusoidal potential perturbation in 100 kHz–10 mHz frequency range.

Surface analysis

The surface of the carbon steel electrodes, before and after their exposure to the studied solutions (with and without inhibitor), was examined with a Philips FEI Quanta 200 scanning electron microscope (SEM) with a tungsten filament with a link to a Genesis X-ray analysis system EDX using an electron acceleration of 20 keV to determine the elemental composition of the films formed onto the electrode surfaces. During analysis, the sample was glued with conductive cement on a stub. The EDX collection time was 100 s.

Steel samples

The specimens used in this investigation were cylindrical discs cut from a carbon steel rod, with the following composition (weight %): C 0.97 %, Si 0.36 %, Mn 0.83 %, Al 0.84 %, and Fe balance.

The discs, with a diameter of 5 mm, were fitted by Teflon on a glass tube as a holder. The specimens were mechanically polished with a series of emery papers up to 1200 grade and then cleaned with distilled water before each experiment. The rotation speed of carbon steel electrodes was adjusted to 1000 rpm.

Results and discussion

Open circuit potential measurements

Open circuit potential is the corrosion potential in the absence of net electrical current flowing to or from the metal surface. Evolution of the corrosion potential versus time constitutes a method for monitoring interface modification between a metal and its environment [29].

The OCP curves of the carbon steel electrode in aerated 3 % NaCl solutions in the absence and presence of different concentrations of TPA are shown in Fig. 2. The potential of carbon steel in chloride solution alone increased to more negative values in the first few minutes of immersion as a result of chloride ion attack on the metal surface. A slight shift in the potential toward the positive direction was recorded with time due to the formation of corrosion products and/or oxide film on the carbon steel surface. This process could lead to a partial protection of carbon steel surface from further dissolution. In the presence of 10^{-4} and $5 \cdot 10^{-4}$ mol L^{-1} TPA solutions, the potential showed almost the same behavior with time but with more absolute positive potential shifts increasing with increase in TPA concentration. This indicates that TPA at these concentrations can reduce the dissolution of carbon steel but still not enough to fully prevent it. Furthermore, the addition of 10^{-3} mol L^{-1} TPA shifted the OCP from the first moment of electrode immersion toward the positive direction. Such OCP behavior reveals that the TPA molecules at 10^{-3} mol L^{-1} concentration might have the ability to form a surface protective layer that gets thicker with time and therefore leads to the positive potential shift. We can conclude that the presence of enough TPA prevents the corrosion of iron through its isolation from being exposed to the corrosive chloride ions. The positive potential shift suggests that the kinetics of the anodic reaction of carbon steel in 3 % NaCl solution was affected strongly in presence of TPA.
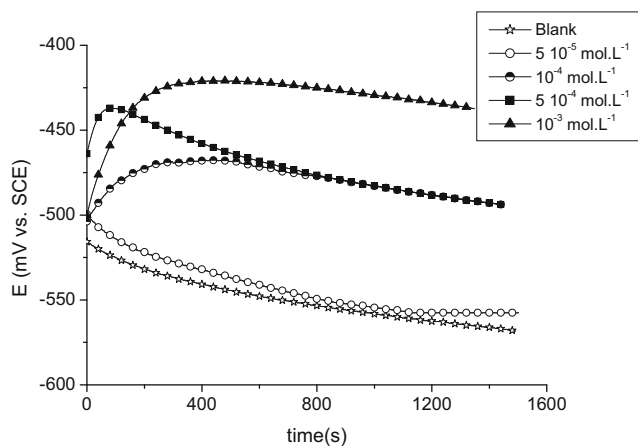
Potentiodynamic polarization

Polarization measurements are commonly accepted to provide relevant information about the kinetics of electrochemical corrosion processes. Figure 3 shows the cathodic and anodic polarization curves recorded for carbon steel, at a rotating disc electrode (rotation speed $\omega = 1000$ rpm) in 3 % NaCl solution in absence and presence of TPA at different concentrations. The samples were immersed in the studied solution for 30 min to stabilize the electrode surface before measurement.

The mechanism of corrosion of carbon steel in nearly neutral aqueous medium is well known. The reactions are as follows:

$$Fe \rightarrow Fe^{2+} + 2\ e^- \qquad (1)$$
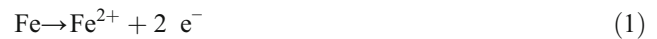
The reaction (1) is induced by Cl^- to form $FeCl_2$ which is further hydrolyzed by water to the hydroxide ($FeCl_2 + 2\ H_2O \rightarrow Fe(OH)_2 + 2H^+ 2Cl^-$)

Fe^{2+} undergoes further oxidation in the presence of oxygen available in the aqueous solution:

$$Fe^{2+} \xrightarrow{[O_2]} Fe^{3+} + 1e^-$$
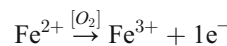
The corresponding reduction reaction at cathodic sites in neutral and alkaline media is

$$O_2 + 2\ H_2O + 4\ e^- \rightarrow 4\ OH^- \qquad (2)$$

Fe^{3+} ions produced in anodic areas and OH^- ions produced in cathodic areas combine to form $Fe(OH)_3$ which is precipitated on the surface of the metal because of its very low solubility. $Fe(OH)_2$ and $Fe(OH)_3$ react further to form the final corrosion products (FeO and Fe_2O_3).

Fig. 2 Change of free corrosion potential of carbon steel in 3 % NaCl containing different concentrations of TPA
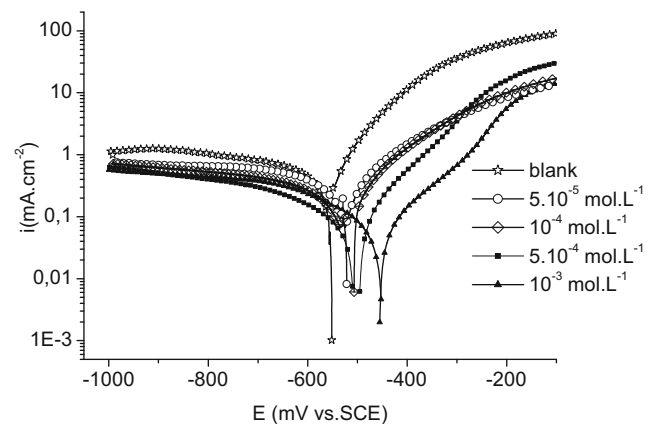

Fig. 3 Anodic and cathodic polarization curves of carbon steel in 3 % NaCl containing different concentrations of TPA

In Fig. 3, we may see that TPA causes a significant decrease in current density (i_{corr}) as a consequence of the blocking effect of inhibitor on the metal surface. The polarization curves illustrate the same trend as that in OCP measurements: addition of inhibitor to electrolyte solution shifts the corrosion potential to a more positive direction. Particularly, it is observed that the addition of the inhibitor suppresses the anodic reaction to a larger extent. In the cathodic range, the current is less sensitive to the TPA concentration. In the absence of TPA, a current plateau appeared from −600 to −1000 mV versus SCE, classically attributed to oxygen reduction under diffusion control in these conditions.

Different approaches have been reported in the literature to determine the corrosion current. It was shown that in the case of the corrosion process which is controlled only by convective diffusion at relatively low rotation speeds (up to 1000 rpm), the corrosion rate can be considered equal to the limiting diffusion current [30]. In the present case, the cathodic process is independent of the TPA concentration. Thus, i_{corr} cannot be extracted from the cathodic branch [31]. In case of anodic inhibitor, where the anodic current exhibits a plateau, its extrapolation allows calculating inhibitive efficiency [32]. However, the estimation of i_{corr} from the anodic branch is not accurate [33]. Due to this lack of accuracy, the corrosion current was determined from the polarization curves by extrapolation of both anodic and cathodic branch. To obtain an accurate measurement of i_{corr}, the study was pursued using electrochemical impedance spectroscopy.

The inhibition efficiency ($\eta\%$) was determined using Eq. 3:

$$\eta\% = \left(1 - \frac{i_{corr}}{i^0_{corr}}\right) \times 100 \qquad (3)$$

where i_{corr} and i^0_{corr} are the corrosion current density values with and without inhibitor, respectively.

The fraction of the surface covered by the adsorbed molecules (θ) was determined from Eq. 4:

$$\theta = \frac{\eta\%}{100} \qquad (4)$$

The values of the corrosion potential (E_{corr}), the corrosion current density (i_{corr}), the corrosion inhibition efficiency ($\eta\%$), and the fraction of the surface covered by the adsorbed molecules (θ) for various TPA concentrations in 3 % NaCl are given in Table 1.

The table shows that the addition of TPA in blank medium is accompanied by a shift of the corrosion potential toward the positive values. Furthermore, the shift was found to depend on inhibitor concentration. The shift of

Table 1 Electrochemical parameters (i_{corr}, E_{corr}, $\eta\%$, and θ) determined from polarization measurements of carbon steel electrode in 3 % NaCl solution in the absence and presence of different concentrations of TPA

Concentration of TPA (mol L^{-1})	E_{corr} (mV$_{SCE}$)	i_{corr} (mA cm^{-2})	η (%)	θ
0	−560	0.416	–	
5×10^{-5}	−555	0.201	52	0.52
10^{-4}	−517	0.176	58	0.58
5×10^{-4}	−510	0.094	77	0.77
10^{-3}	−450	0.051	88	0.88

the corrosion potential in the noble direction is consistent with an effective dependence of the anodic reaction on inhibitor concentration; this illustrates that TPA acts preferentially on the anodic sites and decreases the rate of the anodic iron dissolution [34]. At high concentrations (5· 10^{-4} and 10^{-3} mol L^{-1}), the anodic curves exhibit a passivity plateau. The height of this plateau depends on the inhibitor concentration, indicating an improvement of the protective proprieties of the film when concentration was increased. Similar results were reported in literature for phosphonocarboxylic acid salts (PCAS) [19]. An abrupt current rise at approximately −250 mV is correlated with a breakdown of passivity due to desorption of the inhibiting film. This current rise has been associated with the development of localized corrosion [19]. Such behavior is usually observed for anodic inhibitors and is intensified in solutions containing aggressive ions such as chloride. However, increase in inhibitor concentration produces a better resistance to uniform corrosion, illustrating also that inhibitor content has a beneficial effect. These results give a qualitative indication that a protective film is formed by the inhibitor molecules. This effect can be ascribed to the outcome of a competitive adsorption on the electrode surface between the inhibitor molecules and the chloride ions. In other words, the adsorbed inhibitor molecules on the carbon steel surface can effectively screen the potential sites for the chloride ions adsorption and then act as a barrier to block the adsorption of chloride ions onto metal surfaces [35, 36], and thus retards the destructive action of the Cl$^-$ ions [37]. Apparently, the bond between the surface atoms of metal and the adsorbed inhibitor anions is strong enough to inhibit oxidation [37].

The values of $\eta\%$ obtained from polarization curves indicate that TPA is a more efficient corrosion inhibitor compared to piperidin-1-yl-phosphonic acid (PPA) [38, 39] and (4-phosphono-piperazin-1-yl)-phosphonic acid (PPPA) [39, 40] whose effects on the inhibition of iron corrosion in sodium chloride solutions have been reported in less harsh conditions (rotation speed ω=0 rpm).

EIS measurements

EIS measurements were carried out to investigate the inhibition effect of TPA as well as the kinetics of corrosion reaction process. Figure 4 shows the Nyquist (a, b) and Bode (c, d) plots for carbon steel in 3 % NaCl solutions with and without an inhibitor at OCP immersed for 30 min at $\omega=1000$ rpm. In the absence of TPA (Fig. 4a), the impedance plot exhibited two capacitive loops typical for iron in this corrosive medium. The first loop, at high frequencies (HFs), quite flattened, was associated to the double-layer capacitance, the charge transfer resistance of the corrosion process, and the surface heterogeneity, whereas the low-frequency loop indicates a transport process through the iron oxide layer [1, 41, 42]. Thus, the diameter of the curve must be equal to the polarization resistance value (R_p), which included the charge transfer resistance (R_t) and the diffuse layer resistance (R_d). In this case, the corrosion current is obtained from R_t. It can be observed that the impedance response of the electrode has significantly changed after the addition of TPA in the blank solution (Fig. 4b). It is clear from this figure that in inhibited solution, Nyquist plot yields a slightly depressed semicircular shape, and only one time constant was observed in Bode format. The latter indicates that the corrosion inhibition of the carbon steel in the presence of inhibitor is primarily controlled by a charge transfer process. As previously mentioned, the cathodic

current is controlled by mass transport. Thus, at the corrosion potential, the corresponding faradic impedance in the low-frequency range is very high with respect to the anodic impedance. As a consequence, the polarization resistance (R_p), reported in Table 2, essentially corresponds to the anodic charge transfer resistance (R_t), and in contrast to the non-inhibited situation, polarization resistance measurements can be used to evaluate the corrosion rate [33, 43]. The protective efficiency ($\eta\%$) was determined using the polarization resistance as defined in Eq. 5, where R_t^0 and R_t are the transfer charge resistance in absence and presence of TPA, respectively:

$$\eta\% = \left[\frac{R_t - R_t^0}{R_t}\right] \times 100 \qquad (5)$$

It can be observed that the value of the polarization resistance significantly increased as TPA increased. The diagrams can be fitted by a simple equivalent circuit composed of the electrolyte resistance R_e, in series with the polarization resistance R_p, in parallel with capacitance C_{dl}.

As shown in Fig. 4b, the increase in the diameter of the Nyquist semicircles with increasing concentrations of TPA suggests that the presence of the inhibitor molecules greatly but gradually influences the corrosion kinetics on the electrode surface. Also, in presence of TPA, a continuous increase
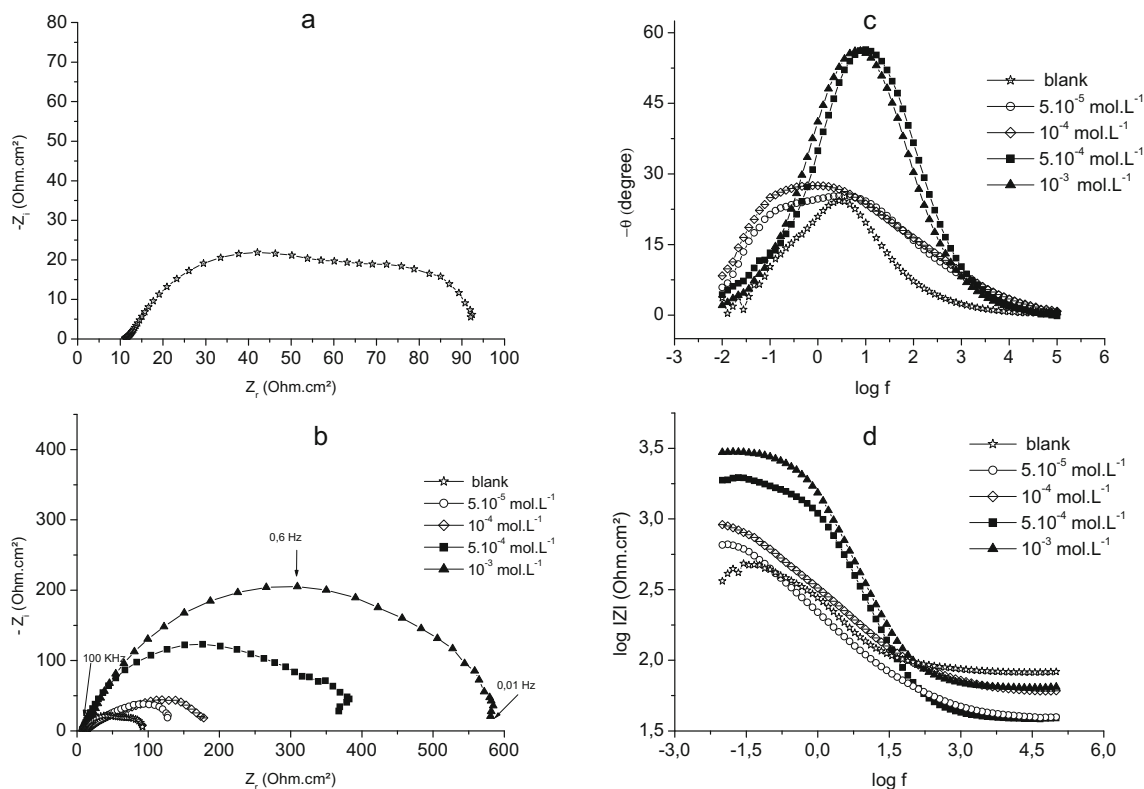

Fig. 4 Nyquist (a, b) and Bode plots—phase angle (c) and impedance modulus (d)—for carbon steel in 3 % NaCl in the absence and the presence of different concentrations of TPA

Table 2 Impedance parameters for carbon steel corrosion in 3 % NaCl without and with TPA at different concentrations

Concentration of TPA (mol L^{-1})	R_t (Ω cm^2)	C_{dl} (μF cm^{-2})	η (%)
0	82	160	–
5×10^{-5}	170	57.93	52
10^{-4}	190	49.92	57
5×10^{-4}	450	55.26	79
10^{-3}	650	31.10	87

in the phase angle shift with increasing concentration was observed. This phase angle shift resulted from the formation of an inhibitor film, which changed the electrode interfacial structure. The continuous increase in the phase angle shift is obviously correlated with the progress of surface coverage by the inhibitor molecules [44, 45].

The high frequency capacitance values were obtained from the slope of a plot of the imaginary component (Z_i) of the impedance at high frequencies versus inverse of frequency between 100 kHz and 100 Hz using the following equation:

$$C_{dl} \rightarrow \frac{1}{Z_i \times \omega} \, as \, \frac{1}{\omega} \rightarrow 0 \qquad (6)$$

As can be seen from Table 2, the value of the charge transfer resistance R_t increased with increasing inhibitor concentration, indicating considerable surface coverage by the inhibitor molecules through strong bonding to the surface [46, 47]. Moreover, the value of C_{dl} decreased with increasing inhibitor concentration, which is probably due to a decrease in local dielectric constant and/or an increase in the thickness of the electrical double layer, suggesting strong adsorption of the inhibitors onto the surface of carbon steel [48]. This fact is undergoes by the displacement of the water molecules by the inhibitor molecules at the interface of the electrical double layer leading to the inhibition of the charge transfer between the solution and metal surface. This behavior could be associated with the adsorption mechanism of the inhibitor at carbon steel/solution interface leading to the formation of a barrier film. The adsorption can occur directly on the basis of donor acceptor interactions between the electrons of oxygen in TPA compound and the vacant d orbital of carbon steel surface atoms. The inhibition efficiencies obtained from EIS and potentiodynamic polarization techniques agree well.

Effect of temperature

To assess the effect of temperature on corrosion inhibition processes, polarization experiments were performed at 20, 30, 40, and 50 °C in uninhibited and inhibited solutions

containing different concentrations of TPA for a 30-min immersion. The various electrochemical parameters derived from these measurements were calculated as in the "Potentiodynamic polarization" section, and the obtained inhibition efficiency (%) was presented as function of temperature in Fig. 5a. It can be seen that η% decreased with increase in temperature; however, the decrease is less pronounced at high TPA concentration. The decrease in η% is less than 20 % at 10^{-3} mol L^{-1} TPA concentration, indicating that TPA can protect the carbon steel against corrosion at all temperature. Even at low TPA concentrations, η% remains at about 15 % at high temperature (Fig. 5a), indicating that the overlaying film is somewhat stable and still protect the carbon steel. For example, Fig. 5b shows the results obtained in the case of 10^{-3} mol L^{-1} TPA. It displays the passivity plateau, discussed in the "Potentiodynamic polarization" section, related to the strength adsorption of TPA on the metal surface, which still remains at higher temperatures. Also, we can see from the data in Fig. 5b that the effect of temperature seems to be very small
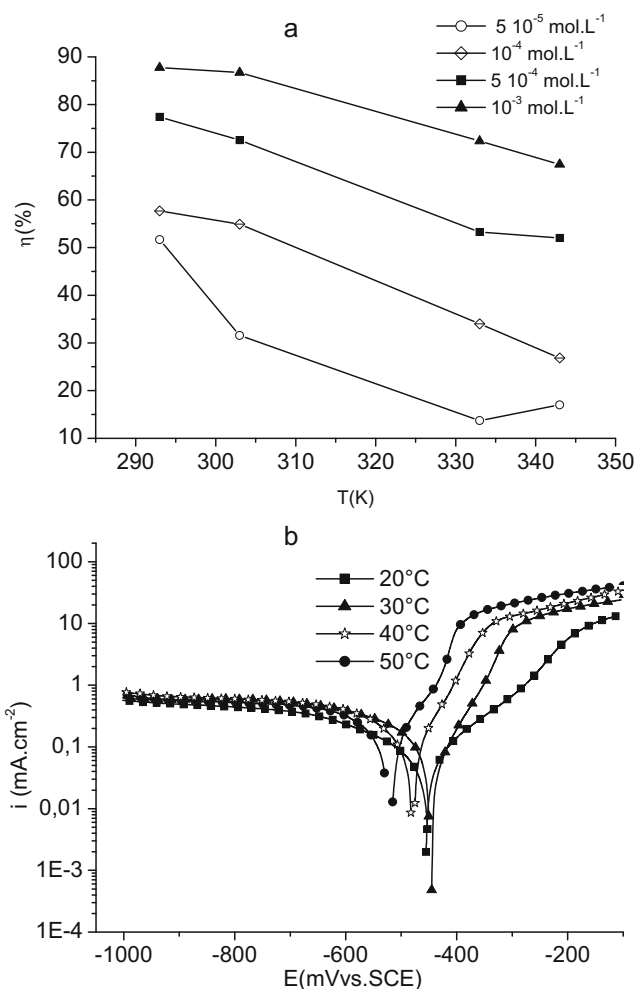

Fig. 5 **a** Effect of temperature on the inhibition efficiency (%) for carbon steel in 3 % NaCl containing TPA in different concentrations. **b** Anodic and cathodic polarization curves of carbon steel in 3 % NaCl with 10^{-3} mol L^{-1} of TPA at different temperatures

in the cathodic branch compared with anodic one. Thus, the decrease in current efficiency can be attributed to desorption of the TPA molecules as the temperature increases rather than an increase of the oxygen supply to the metal surface.

The adsorption of an organic inhibitor can affect the corrosion rate by either decreasing the available reaction area (geometric blocking effect) or by modifying the activation energy of the anodic or cathodic reactions occurring in the inhibitor-free surface in the course of the inhibited corrosion process. The Arrhenius-type relationship between the corrosion rates of carbon steel in 3 % NaCl media (Eq. 7) was used to determine the activation energies (E_a):

$$i_{corr} = Ae^{-\frac{E_a}{RT}} \qquad (7)$$

where E_a is the activation energy, A is the pre-exponential factor, R is the universal gas constant, and T is the absolute temperature. The apparent activation energy and pre-exponential factor can be calculated from the slope and intercept of the Arrhenius plots (log i_{corr} vs. 1/T; Fig. 6). All kinetic parameters were calculated and listed in Table 3. The apparent activation energy, at relative lower concentration ($5 \cdot 10^{-5}$ and $5 \cdot 10^{-4}$ mol L^{-1}), increases with increasing concentrations of TPA, while it decreases at 10^{-3} mol L^{-1}. That is to say, in this system, there is a maximum for the apparent activation energy. The result is the same as the results of other studies [49, 50], probably meaning that the chemical adsorption takes place at a high concentration. We may remark that the variation in the pre-exponential factor is similar to the variation in the apparent activation energy.

A decrease in η% with rise in temperature, with analogous increase in corrosion activation energy in the presence of TPA compared with its absence, is frequently interpreted as being suggestive of formation of an adsorption film of a physical
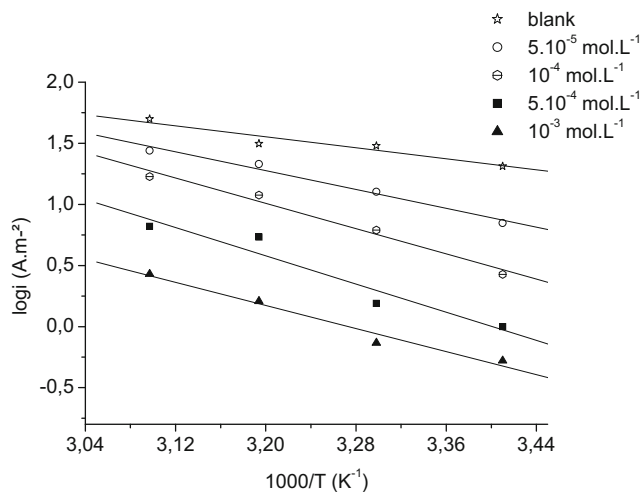
Table 3 Kinetic parameters of the corrosion rate of carbon steel in 3 % NaCl without and with TPA at different concentrations

Concentration of TPA (mol L^{-1})	A	E_a (kJ mol^{-1})	Linear correlation coefficient
0	46.98	1.76	0.87
5×10^{-5}	1660	6.12	0.97
10^{-4}	17961	22.88	0.98
5×10^{-4}	17961	23.95	0.93
10^{-3}	2435	19.82	0.96

character [51]. According to Gomma [52], the kinetics of such corrosion process acquires the character of a diffusion process in which, at lower temperature, the quantity of inhibitor present at the metal surface is greater than that at higher temperatures. The high-temperature disruption of the system is sufficiently minimized at high TPA concentration, and the inhibiting effect is more or less stable (Fig. 5b). This is probably because TPA becomes present in sufficient amounts to chemically interact with the metal surface, hence improving the stability of the inhibiting TPA layer formed by physical adsorption and modifying the corrosion activation energy. Accordingly, TPA can be chemically adsorbed on the carbon steel surface and exert a controlling influence on the corrosion inhibition performance. Chemisorbed molecules are thought to provide more effective protection than physisorbed ones, since they reduce the inherent reactivity of the metal at the sites where they are attached. This effect is enhanced with rise in temperature, leading to greater surface coverage and hence to less pronounced decreasing inhibition efficiency.

Adsorption isotherm

In order to obtain more information about the interaction between the TPA molecules and the carbon steel surface, different adsorption isotherms were tested. The adsorption on the corroding surfaces never reaches the real equilibrium and tends to reach an adsorption steady state. When the corrosion rate is sufficiently decreased in the presence of inhibitor, the adsorption steady state has a tendency to attain quasi-equilibrium state. In this case, it is reasonable to consider the quasi-equilibrium adsorption in thermodynamic way using the appropriate equilibrium isotherms [53]. Quasilattice models consider the surface of the metal in aqueous solution to be covered with water dipoles, and for the adsorption of organic molecules to occur, these water dipoles must be replaced by organic molecules

The best fit straight line was obtained for a plot of C/θ (mol L^{-1}) versus C (mol L^{-1}) with a slope of around unity. The correlation coefficient (r^2) was used to choose the isotherm type that best fit the experimental data. These plots

Fig. 6 Relation between corrosion rate and reciprocal of temperature for carbon steel in 3 % NaCl containing different concentrations

suggest that the adsorption of TPA on the carbon steel surface follows the Langmuir adsorption isotherm (Fig. 7), which can be represented by Eq. 8:

$$\frac{\theta}{1-\theta} = KC \qquad (8)$$

where K represents the constant of adsorption reaction, C is the concentration of inhibitor, and θ is the surface coverage obtained from the following equation:

$$\theta = \left(1 - \frac{i_{corr}}{i_{corr}^0}\right) \qquad (9)$$

The values of i_{corr} were determined from polarization measurements. The value of equilibrium constant, K, was calculated from the reciprocal of the intercept of isotherm line as $1.6 \cdot 10^4$ L mol^{-1} at 293 K. This high value of K indicates that the inhibitor possesses strong adsorption ability onto the carbon steel surface [54].

Thermodynamic parameters

The thermodynamic model can be used to explain the adsorption phenomenon of the inhibitor molecule. Using the obtained adsorption coefficients, adsorption free energy, adsorption heat, and adsorption entropy can be calculated.

The adsorption heat was calculated according to the Van't Hoff Eq. (10) [54]:

$$\ln K = \frac{-\Delta H}{RT} - \left(-\frac{\Delta S}{R} + \ln 55.5\right) \qquad (10)$$

where T is the temperature and the constant value 55.5 represents the concentration of water in solution in mol L^{-1}.
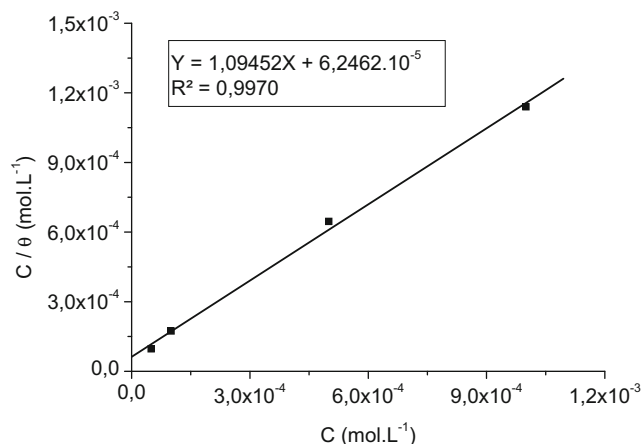
The calculated values of the adsorption constant $\ln K$ were plotted as a function of reciprocal temperature T^{-1}, and a straight line was obtained, as shown in Fig. 8. The adsorption heat(ΔH) and adsorption entropy (ΔS) can be obtained by using the slope values of ($\Delta H/R$) and the intercept of the curve of [(ln 55.5) − (ΔS/R)]. Under the experimental conditions, the adsorption heat can be approximately regarded as the standard adsorption heat (ΔH). According to the thermodynamic basic equation $\Delta G = \Delta H - T \times \Delta S$, the standard adsorption free energy (ΔG) could be calculated for each temperature.

All thermodynamic parameters obtained are listed in Table 4. The negative values for ΔG (Table 4) reveal the spontaneity of the adsorption process and the stability of the adsorbed layer on the carbon steel surface [55]. According to Noor [56], if $|\Delta G| \leq$ 20 kJ mol^{-1}, the interaction between the inhibitor and the charged metal surface is electrostatic in nature (physisorption), whereas if $|\Delta G| \geq 40$ kJ mol^{-1}, the interaction is of the charge transfer type (chemisorption).

In our study, ΔG was approximately −33 kJ mol^{-1} at 298 K and increased in magnitude (i.e., became more negative) with increasing temperature. This reveals that the adsorption of TPA on the carbon steel surface takes place through mixed-type adsorption including both chemical and physical adsorption [57, 58]. As the temperature increased, the inhibition efficiency of TPA decreased, which might be due to the disappearance of electrostatic interaction between the metal surface and the π electrons of the inhibitor molecules. The fact that the ΔG values increased in magnitude with temperature indicate that the adsorption of inhibitors is more spontaneous with increasing temperature. The negative values of ΔH reflect the exothermic nature of the adsorption process on carbon steel. The positive values for the entropy of activation can be attributed to the increase in the solvent entropy [39].
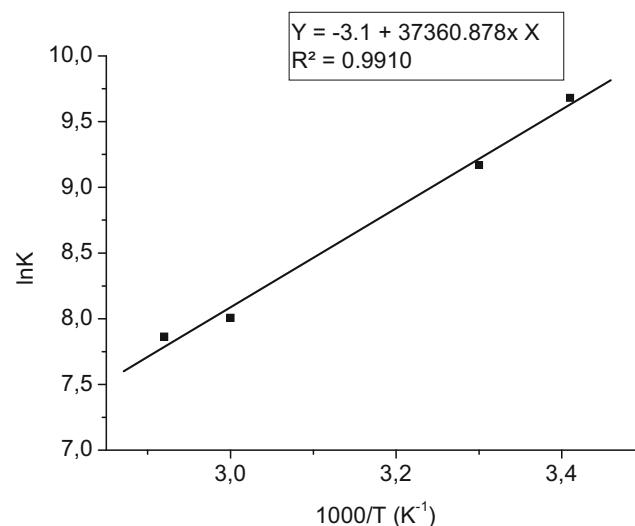

Fig. 7 Langmuir's adsorption plots for carbon steel in 3 % NaCl containing different concentrations of TPA at 20 °C

Fig. 8 Arrhenius plots of ln$K$ against $1/T$ for carbon steel in 3 % NaCl solution

Table 4 Thermodynamic parameters of adsorption isotherm of TPA on the carbon steel surface at different temperatures

| T (K)	$K \times 10^{-4}$	ΔG (kJ mol^{-1})	ΔH (kJ mol^{-1})	ΔS (J mol^{-1} K^{-1})
293	1.6	−33.23	−31	7.61
303	0.96	−33.32		
333	0.3	−33.55		
343	0.26	−33.62		

Surface characterization

Figure 9 shows the SEM surface morphology of carbon steel electrode after 1 day of immersion in aerated 3 % NaCl containing solution in the absence and presence of TPA. For comparison, a SEM image of polished steel surface (control sample) is shown in Fig. 9a. The image of the surface exposed to the inhibitor free solution (Fig. 9c) is strongly corroded by the medium, resulting in a porous, rough, and heterogeneous surface of corrosion products with a granular structure. The crystals are lath-like, the shape commonly reported for iron oxides as lepidocrocite. In contrast, in the presence of the inhibitor (Fig. 9e), improvement in the carbon steel surface is observed and the formation of an inhibitor layer is revealed, which further confirms the inhibition action.

The corresponding EDX spectra are shown in the absence and presence of TPA (Fig. 9b, d, f). The EDX analysis performed on the surface of the control sample (polished surface; Fig. 9b) shows the presence of peaks attributed to Fe and C, specific elements of the steel. In chloride solution alone (Fig. 9d), the carbon steel surface contains mainly Fe and O with small quantities of Na and Cl. This indicates that the

Fig. 9 SEM images and their corresponding EDX analysis of carbon steel before immersion (**a**, **b**), after 1 day of immersion in 3 % NaCl (**c**, **d**), and after 1 day of immersion in 3 % NaCl containing 10^{-3} mol L^{-1} of TPA (**e**, **f**)
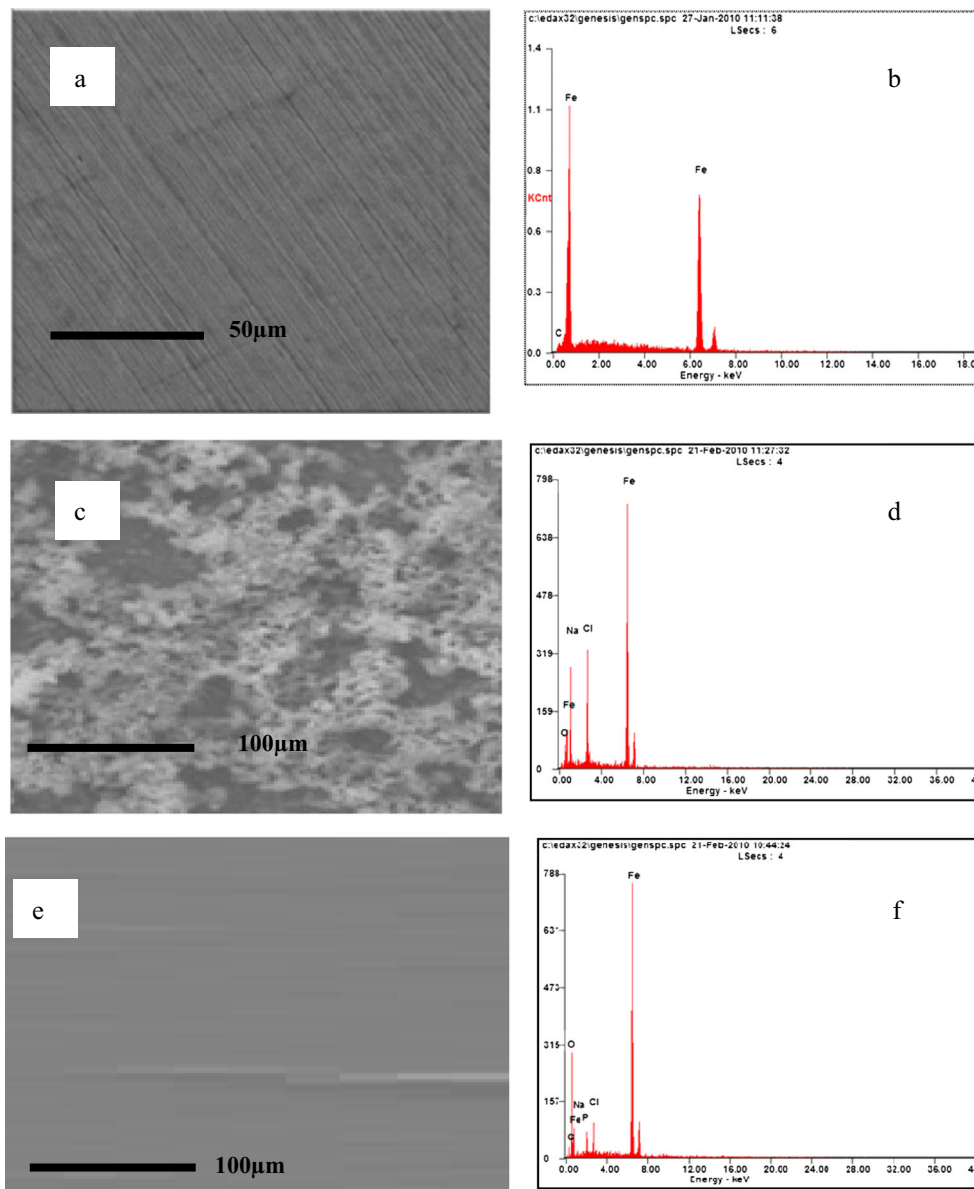
corrosion of iron took place through the formation of iron oxides and/or iron chlorides. On the other hand, the elements found in the adsorbed layer obtained by EDX in the presence of TPA inhibitor (Fig. 9f) were carbon, oxygen, and phosphorus, beside the iron substrate in addition to a very low content of chlorine. The detection of C, O, and P on the surface indicates undoubtedly the presence TPA molecules on the carbon steel surface. The oxygen peak which appears in this case is not assigned to an iron oxide or iron hydroxide, but it is rather assigned to the inhibitor composition as shown in Fig. 1. The presence of TPA on the surface could lead to the positive shifts of OCP and E_{corr}, shown in Figs. 2 and 3 and in Table 1, respectively, in the presence of TPA and with the increase of its concentrations. The appearance of low content of chlorine in the EDX profile confirms that TPA molecules preclude the corrosion of iron through its strong adsorption on the surface blocking its weak damages and preventing the formation of ferrous and ferric chloride compounds.

Mechanism of inhibition

It is well recognized that organic inhibitor molecules set up their inhibition action via the adsorption of the inhibitor molecules onto the metal/solution interface. The adsorption process is affected by the chemical structures of the inhibitors, the nature and surface charge of the metal, and the distribution of charge over the whole inhibitor molecule. The adsorption can occur on the metal surface in one or more of the following ways:

(a) Electrostatic interaction between the charged molecules and the charged metal
(b) Interaction of unshared electron pairs in the molecule with the metal
(c) Interaction of π-electrons with the metal
(d) A combination of types (a–c) [59, 60]

Based on the above thermodynamic results, the adsorption of TPA on the carbon steel surface cannot be considered only as purely physical or as purely chemical adsorption phenomenon.

It is well known that steel surface is positively charged in NaCl as the values of E_{corr} are more positive than the corresponding values of potential of zero charge (PZC) [61]. Furthermore, TPA has acid character and expected to be deprotonated [28] in equilibrium with the corresponding neutral form in NaCl neutral solutions. Thus, it is easy for the negatively charged inhibitors to approach the positively charged steel surface due to the electrostatic attraction and then act as a barrier to block the adsorption of chloride ions onto metal surfaces.

In addition to the physical adsorption, a chemical adsorption can occur during the process of inhibitor adsorption on

metal surfaces. The possible reaction centers are unshared electron pair of heteroatoms and π-electrons of aromatic ring. The adsorption can be explained on the basis of the donor-acceptor interaction between π-electrons of donor atoms (P) and (O) from functional group (PO(OH)$_2$), of the inhibitors and the vacant d orbitals of iron surface atoms [57, 59, 60].

The hydroxyl group (−OH), which is an electron donor, moderately activated by virtue of presence of lone pair of electrons on the oxygen (O) atom, can lead to the increase of the electron density on the phosphonic group (PO(OH)$_2$).

In addition, the rigidity of π-delocalized system of TPA may increase or decrease the electron density on the adsorption center; therefore, it is leading to an easier electron transfer from the functional group (−OH group) to the metal surface, strengthening coordinate bonding and leading to different adsorption centers and corrosion inhibition efficiency. Between the two possibilities, the chemisorption mode is likely predominant due to the rather high value of ΔG obtained. The fact that TPA has four phosphonic groups means that it can be anchored to the surface at 4 points, meaning a fourfold stronger bonding per molecule leading to parallel adsorption to the metal surface.

Finally, it should also be emphasized that the large size and high molecular weight of TPA molecule can also contribute the greater inhibition efficiency due to large area coverage

Conclusions

The corrosion inhibition of carbon steel by a newly synthesized tetraphosphonic acid (TPA) was studied by electrochemical measurements and surface analysis, and the obtained results show that

(i) The inhibition efficiency on carbon steel in 3 % NaCl solution increases with increasing concentrations of TPA inhibitor. The maximum inhibition efficiency of 88 % was observed at l0^{-3} mol L^{-1} concentration.
(ii) The compound acts as an anodic type inhibitor through the formation of protective adsorption layer on the carbon steel surface, which can sufficiently hinder the access of chloride ions to the metal surface and suppress the chloride induced corrosion in solution.
(iii) The adsorption of the inhibitor obeys the Langmuir adsorption isotherm via a strong mixed chemical and physical interaction with the carbon steel surface.
(iv) The calculated Gibbs free energy value indicates the mixed physical/chemical interaction with the carbon steel surface.
(v) SEM and EDX analysis of the carbon steel surface showed that a film of inhibitor is formed on the carbon steel surface, which can sufficiently hinder the access of

chloride ion to the metal surface and suppress the chloride-induced corrosion in 3 % NaCl solution.

(vi) The corrosion inhibition efficiency decreased with increasing temperature but the decrease is less pronounced at high TPA concentration in the solution, implying that TPA keeps its effectiveness with temperature. The decrease in $\eta\%$ is less than 20 % at 10^{-3} mol L^{-1} TPA concentration.

All these results show clearly that TPA is a good corrosion inhibitor of carbon steel in aerated 3 % NaCl solutions.

References

1. Hammache H, Makhloufi L, Saidani B (2003) Corrosion protection of iron by polypyrrole modified by copper using the cementation process. Corros Sci 45:2031–2042

2. Benchikh A, Aitout R, Makhloufi L, Benhaddad L, Saidani B (2009) Soluble conducting poly(aniline-co-orthotoluidine) copolymer as corrosion inhibitor for carbon steel in 3% NaCl solution. Desalination 249:466–474

3. McCoy JW (1983) Chemical treatment of cooling water, 2nd edn. Chemical Publishing Co., New York, p 147

4. Rajendran S, Apparao BV, Palaniswamy N, Periasamy V, Karthikeyan G (2001) Corrosion inhibition by strainless complexes. Corros Sci 43:1345–1354

5. Gledhill WE, Feitjel TCJ, Hutzinger IO (eds) (1992) The handbook of environmental chemistry, part F, vol. 3. Springer Verlag, Berlin

6. Landner L, Walterson E (1993) Phosphonates used for detergent applications. Swedish Environmental Research Group (MFG), Stockholm

7. Jaworska J, Van-Genderen-Takken H, Hanstvert A, Plassche EVD, Feijtel T (2002) Environmental risk assessment of phosphonates, used in domestic laundry and cleaning agents in the Netherlands. Chemosphere 47:655–665

8. Demadis KD, Katarachia D (2004) Metal-phosphonate chemistry: synthesis, crystal structure of calcium-amino-tris-(methylene phosphonate) and inhibition of $CaCO_3$ crystal growth. Phosphorus Sulfur Silicon Relat Elem 179:627–648

9. Demadis KD, Lykoudis P (2005) Chemistry of organophosphonate scale growth inhibitors: 3. Physicochemical aspects of 2-phosphonobutane-1,2,4-tricarbonate (PBTC) and its effect on $CaCO_3$ crystal growth. Bioinorg Chem Appl 3:135–149

10. Holy AJ, Günter J, Dvorakova H, Masojidkova M, Andrei G, Snoeck R, Balzarini J, de Clercq E (1999) Structure-antiviral activity relationship in the series of pyrimidine and purine N-[2-(2-phosphonomethoxy)ethyl] nucleotide analogues. 1. Derivatives substituted at the carbon atoms of the base. J Med Chem 42:2064–2084

11. Grison C, Letondor C, Chibli H, Coutrot P (2005) One-pot carbanionic access to methylenebis(phosphonate) analogues of natural P1, P2-glycosyl-disubstituted pyrophosphates. Tetrahedron Lett 46:6525–6528

12. Cai ZR, Jabri SY, Jin H, Kim CU, Metobo SE, Mish MR, Pastor RM (2007) Antiviral phosphonate conjugates for inhibition of HIV, Int Patent WO2007014352, Int class: A61K31/662; A61K47/48

13. Darling D, Rakshpal R (1998) Green chemistry applied to corrosion and scale inhibitors. Mater Perform 37:42–45

14. Andijani I, Turgoose S (1999) Studies on corrosion of carbon steel in deaerated saline solutions in presence of scale inhibitor. Desalination 123:223–231

15. Ramesh S, Rajeswari S (2005) Evaluation of inhibitors and biocide on the corrosion control of copper in neutral aqueous environment. Corros Sci 47:151–169

16. Rajendran S, Apparao BV, Palaniswamy N, Amalraj AJ, Sundaravadivelu M (2002) The role of phosphonates as transporters of Zn^{2+} ions in the inhibition of carbon steel in neutral solutions containing chlorides. Anti-Corros Methods Mater 49:205–209

17. Gunasekaran G, Natarajan R, Muralidharan VS, Palaniswamy N, Apparao BV (1997) Inhibition by phosphonic acids. Anti-Corros Methods Mater 44:248–259

18. Balaban-Irmenin YV, Rubashov AM, Fokina NG (2006) Protection of metals. Prot Met 42:133–136

19. Ochoa N, Baril G, Moran F, Pébère N (2002) Study of the properties of a multi-component inhibitor used for water treatment in cooling circuits. J Appl Electrochem 32:497–504

20. Ochoa N, Moran F, Pébère N (2004) The synergistic effect between phosphonocarboxylic acid salts and fatty amines for the corrosion protection of a carbon steel. J Appl Electrochem 34:487–493

21. Nakayama N (2000) Inhibitory effects of nitrilotris(methylenephosphonic acid) on cathodic reactions of steels in saturated $Ca(OH)_2$ solutions. Corros Sci 42:1897–1920

22. Garcia C, Gourbin G, Ropital F, Fiaud C (2001) Study of the scale inhibition by HEDP in a channel flow cell using a quartz crystal microbalance. Electrochim Acta 46:973–985

23. Starostina M, Smorodin A, Gal-Or L (1999) Inhibition by phosphates of mild steel and cast iron in cooling water. Mater Perform 38:52–58

24. Cushner MC, Melchior WC, Przybylinski JL (1990) Effect of iron(II) on the performance of calcium carbonate inhibitors. Mater Perform 29:49–56

25. Sekine I, Hirakawa Y (1986) Effect of 1-hydroxyethylidene-1,1-diphosphonic acid on the corrosion of SS 41 steel in 3% sodium chloride solution. Corrosion 42:272–277

26. Touir R, Dkhireche N, Touhami ME, Sfaira M, Senhaji O, Robin JJ, Boutevin B, Cherkaoui M (2010) Operational parameters effect of sodium gluconate inhibition used in the protection of cooling water system. Mater Chem Phys 122:1–9

27. Aliouane N, Chafaa S, Douadi T, Helesbeux JJ, Khan MA, Bouet G, Duval O (2011) Synthesis of new benzylic di-, tri-, and tetraphosphonic acids as potential chelating agents. Phosphorus Sulfur Silicon 186:354–364

28. Aliouane N, Chafaa S, Douadi T, Helesbeux JJ, Khan MA, Duval O, Bouet G (2010) Novel polydentate phosphonic acids: protonation and stability constants of complexes with Fe(III) and Cu(II) in aqueous medium. Heteroat Chem 2:51–62

29. Felhosi I, Telegdi J, Palinkas G, Kalman E (2002) Kinetics of self-assembled layer formation on iron. Electrochim Acta 47:2335–2340

30. Duprat M, Bui N, Dabosi F (1978) Sur le choix d'un critère de détermination de la vitesse de corrosion d'un acier au carbone dans une solution à 3% de chlorure de sodium aérée et agitée. J Appl Electrochem 8:455–465

31. Ochoa N, Moran F, Pébère N, Tribollet B (2005) Influence of flow on the corrosion inhibition of carbon steel by fatty amines in association with phosphonocarboxylic acid salts. Corros Sci 47:593–604

32. Bommersbach P, Alemany-Dumont C, Millet JP, Normand B (2005) Formation and behaviour study of an environment-friendly corrosion inhibitor by electrochemical methods. Electrochim Acta 5:1076–1084

33. Srisuwan N, Ochoa N, Pébère N, Tribollet B (2008) Variation of carbon steel corrosion rate with flow conditions in the presence of an inhibitive formulation. Corros Sci 50:1245–1250

34. Bentiss F, Traisnel M, Lagrenee M (2000) The substituted 1,3,4-oxadiazoles: a new class of corrosion inhibitors of mild steel in acidic media. Corros Sci 42:127–146

35. Valek L, Martinez S, Mikulic D, Brnardic I (2008) The inhibition activity of ascorbic acid towards corrosion of steel in alkaline media containing chloride ions. Corros Sci 50:2705–2709

36. Martinez S, Valek L, Oslakovic IS (2007) Adsorption of organic anions on low-carbon steel in saturated Ca(OH)$_2$ and the HSAB principle. J Electrochem Soc 154:C671–C677

37. Touir R, Cenoui M, El Bakri M, Ebn Touhami M (2008) Sodium gluconate as corrosion and scale inhibitor of ordinary steel in simulated cooling water. Corros Sci 50:1530–1537

38. Amar H, Tounsi A, Makayssi A, Derja A, Benzakour J, Outzourhit A (2007) Corrosion inhibition of Armco iron by 2-mercaptobenzimidazole in sodium chloride 3% media. Corros Sci 49:2936–2945

39. Amar H, Benzakour J, Derja A, Villemin D, Moreau B (2003) A corrosion inhibition study of iron by phosphonic acids in sodium chloride solution. J Electroanal Chem 558:131–139

40. Amar H, Benzakour J, Derja A, Villemin D, Moreau B, Braisaz T (2006) Piperidin-1-yl-phosphonic acid and (4-phosphono-piperazin-1-yl) phosphonic acid: a new class of iron corrosion inhibitors in sodium chloride 3% media. Appl Surf Sci 252:6162–6172

41. Lenderink HJW, Linden MVD, Wit JHW (1993) Corrosion of aluminium in acidic and neutral solutions. Electrochim Acta 38:1989–1992

42. Garrigues L, Pébère N, Dabosi F (1996) An investigation of the corrosion inhibition of pure aluminum in neutral and acidic chloride solutions. Electrochim Acta 41:1209–1215

43. Bonnel A, Dabosi F, Deslouis C, Duprat M, Keddam M, Tribollet B (1983) Corrosion study of a carbon steel in neutral chloride solutions by impedance techniques. J Electrochem Soc 130:753–761

44. Tan YJ, Bailey S, Kinsella B (1996) An investigation of the formation and destruction of corrosion inhibitor films using electrochemical impedance spectroscopy (EIS). Corros Sci 38:1545–1561

45. Goncalves RS, Azambuja DS, Serpa-Lucho AM (2002) Electrochemical studies of propargyl alcohol as corrosion inhibitor for nickel, copper, and copper/nickel (55/45) alloy. Corros Sci 44:467–479

46. Mernari B, Elattari H, Traisnel M, Bentiss F, Lagrenee M (1998) Inhibiting effects of 3,5-bis(n-pyridyl)-4-amino-1,2,4-triazoles on the corrosion for mild steel in 1 M HCl medium. Corros Sci 40:391–399

47. Ramesh SV, Adhikari AV (2009) N′-[4-(diethylamino)benzylidine]-3-{[8-(trifluoromethyl) quinolin-4-yl]thio}propano hydrazide) as an effective inhibitor of mild steel corrosion in acid media. Mater Chem Phys 115:618–627

48. Kumar SLA, Gopiraman M, Kumar MS, Sreekanth A (2011) 2-Acetylpyridine-N(4)-morpholine thiosemicarbazone (HAcpMTSc) as a corrosion inhibitor on mild steel in HCl. Ind Eng Chem Res 50:7824–7832

49. Tang LB, Mu G, Liu G (2003) The effect of neutral red on the corrosion inhibition of cold rolled steel in 1.0 M hydrochloric acid. Corros Sci 45:2251–2262

50. Li X, Tang L (2005) Synergistic inhibition between OP and NaCl on the corrosion of cold-rolled steel in phosphoric acid. Mater Chem Phys 90:286–297

51. Oguzie EE (2008) Evaluation of the inhibitive effect of some plant extracts on the acid corrosion of mild steel. Corros Sci 50:2993–2998

52. Gomma GK (1998) Corrosion inhibition of steel by benzotriazole in sulphuric acid. Mater Chem Phys 56:27–34

53. Oguzie EE, Unaegbu C, Ogukwe CN, Okolue BN, Onuchukwu AI (2004) Inhibition of mild steel corrosion in sulphuric acid using indigo dye and synergistic halide additives. Mater Chem Phys 84:363–368

54. Ali SA, Al-Mualllem HA, Rahman SU, Saeed MT (2008) Bis-isoxazolidines: a new class of corrosion inhibitors of mild steel in acidic media. Corros Sci 50:3070–3077

55. Abdallah M (2002) Rhodanine azosulpha drugs as corrosion inhibitors for corrosion of 304 stainless steel in hydrochloric acid solution. Corros Sci 44:717–728

56. Noor EA (2007) Temperature effects on the corrosion inhibition of mild steel in acidic solutions by aqueous extract of fenugreek leaves. Int J Electrochem Sci 2:996–1017

57. Ahamad I, Prasad R, Quraishi MA (2010) Inhibition of mild steel corrosion in acid solution by Pheniramine drug: Experimental and theoretical study. Corros Sci 52:3033–3041

58. Gopiraman M, Selvakumaran N, Kesavan D, Kim IS, Karvembu R (2012) Chemical and physical interactions of 1-benzoyl-3,3-disubstitute thiourea derivatives on mild steel surface-corrosion inhibition in acidic medium. Ind Eng Chem Res 51:7910–7922

59. Schweinsberg DP, George GA, Nanayakkara AK, Steiner DA (1988) The protective action of epoxy resins and curing agents-inhibitive effects on the aqueous acid corrosion of iron and steel. Corros Sci 28:33–42

60. Shorky H, Yuasa M, Sekine I, Issa RM, El-Baradie HY, Gomma GK (1998) Corrosion inhibition of mild steel by Schiff base compounds in various aqueous solutions: part 1. Corros Sci 40:2173–2186

61. Zhou X, Yang H, Wang F (2012) Investigation on the inhibition behavior of a pentaerythritol glycoside for carbon steel in 3.5% NaCl saturated Ca(OH)$_2$ solution. Corros Sci 54:193–200